JOURNAL OF AIRCRAFT
Vol. 40, No. 4, July–August 2003

Nonlinear Random Response of Panels in an Elevated Thermal-Acoustic Environment

Jean-Michel Dhainaut,* Xinyun Guo,† and Chuh Mei‡
Old Dominion University, Norfolk, Virginia 23529-0247
and
S. Michael Spottswood§ and Howard F. Wolfe¶
U.S. Air Force Research Laboratory/VASS, Wright–Patterson Air Force Base, Ohio 45433

Sonic fatigue is generally considered as being one of the major design areas for the newest generation of high-speed flight vehicles. Efficient analysis methods for predicting nonlinear random response and fatigue life are urgently needed. This paper presents a finite element formulation for the prediction of nonlinear random response of thin isotropic/composite panels subjected simultaneously to high acoustic loads and elevated temperatures. Laminated plate theory and von Karman large displacement relations are used to derive the nonlinear equations of motion for an arbitrarily laminated composite panel subjected to combined acoustic and thermal loads. The nonlinear equations of motion in physical degrees of freedom are transformed to a set of coupled nonlinear equations in truncated modal coordinates, retaining fewer degrees of freedom. Numerical integration is employed to obtain the panel response to simulated Gaussian band-limited white noise. To validate the formulation, results are compared with existing linear and nonlinear solutions to assess the accuracy of nonlinear modal stiffness matrices and simulated random loads. Examples are given for an isotropic panel at various combinations of sound pressure levels and temperatures. Numerical results include rms values of maximum deflection and strain, time histories of deflection and strain response, probability distribution functions, power spectrum densities, and higher statistical moments. Numerical results predicted all three types of panel motions for a thermal buckled simply supported isotropic plate: linear random vibration about one of the buckled equilibrium position, snap-through motions between the two buckled positions, and nonlinear random response over both buckled positions.

Introduction

RESURGENT interest in high-speed flight vehicles necessitates further development of sonic fatigue technology.[1,2] The surface thermal protection systems (TPS) of advanced high-speed aircraft and spacecraft, such as the reusable launch vehicle, the X-43 Hyper-X program, and the Quiet Supersonic Platform, etc., will be constructed from high-temperature-resistant composite or superalloy materials. The major advantages that composite materials provide are the increased strength-to-weight ratio and the higher structural damping over superalloy structures. The higher damping values would help yield smaller dynamic response and strain, thus enhancing fatigue life. The TPS would exhibit large displacements under high acoustic loads and possibly display buckling at elevated temperatures. Both of these effects are nonlinear in nature and make prediction of fatigue life extremely difficult.[1–3] Reliable experimental data are difficult to acquire because of the high costs and difficulties with instrumentation at high acoustic intensity and elevated temperature. Thus, in the design process greater emphasis will likely be placed on improved mathematical and computational prediction methods.

There are five major analysis methods for the prediction of nonlinear response of structures: 1) perturbation, 2) Fokker–Plank–Kolmogorov (FPK equation), 3) Monte Carlo, 4) equivalent linearization (EL), and 5) finite element (FE) numerical integration. The perturbation technique[4] has been shown that it is limited to weak geometric nonlinearities, and the FPK equation approach[5] yields to an exact solution only for single-degree-of-freedom (DOF) systems. Monte Carlo simulation[6,7] is the most general method, but the use of partial differential equation and Galerkin's approach limits its applicability to rather simple structures.[8–10] Equivalent linearization methods have been widely applied because of their ability to capture accurately the response statistics over a wide range of response while maintaining a relatively light computational burden.[11,12] The drawback of the equivalent linearization technique is the assumption that the response has to be Gaussian. For the finite element numerical integration method[13,14] the computational cost is the main concern because the finite element model often includes hundreds, if not thousands, number of physical DOFs, and the nonlinear terms are updated and reassembled at each time step.

The application of the finite element and EL methods was extended to structures subjected to thermal and acoustic loads.[15–17] The thermal postbuckling structural problem was solved first to obtain the deflection and thermal stresses, they were then treated as known preconditions for the subsequent random response analysis. The known preconditions dealt with only one of the two postbuckling positions; therefore, the FE/EL approach does not give accurate predictions for snap-through and large nonlinear random motions. This paper presents a new analytical method for the prediction of nonlinear random response of composite panels at elevated temperatures. The system equations of motion are first derived in the physical DOF using the finite element approach. Then they are reduced to a set of coupled nonlinear modal equations. Numerical integration is used to obtain the panel response. All of the three types of motion—1) linear random vibration about one of the two buckled positions, 2) snap-through motion between the two buckled positions, and 3) nonlinear random vibration over the two thermally buckled positions—can be predicted. Examples for an isotropic plate at various combinations of sound pressure level and temperature are given.

Received 24 October 2001; revision received 12 January 2003; accepted for publication 17 February 2003.

*Graduate Student, Department of Aerospace Engineering.
†Graduate Student, Department of Aerospace Engineering. Student Member AIAA.
‡Professor, Department of Aerospace Engineering, 241 Kaufman Hall; cmei@odu.edu. Associate Fellow AIAA.
§Aerospace Engineer, Structural Dynamics Branch. Member AIAA.
¶AFRL Retired, Structural Dynamics Branch. Senior Member AIAA.

Finite Element Formulation

The governing nonlinear equations of motion are derived for an arbitrarily laminated composite plate subjected to a set of simultaneously applied thermal and acoustic loads. The thermal load is taken to be an arbitrary distribution and steady state, that is, $\Delta T(x, y, z)$. The acoustic excitation is assumed to be a band-limited Gaussian noise and uniformly distributed over the structural surface.

Equations of Motion in Physical DOF

The element displacements are expressed in terms of the node DOF as

$$u(x, y, t) = \lfloor H_u \rfloor \{w_m\}, \qquad v(x, y, t) = \lfloor H_v \rfloor \{w_m\}$$
$$w(x, y, t) = \lfloor H_w \rfloor \{w_b\} \tag{1}$$

where u, v, and w are the in-plane and transverse displacements of the middle surface; the vectors $\{w_m\}$ and $\{w_b\}$ denote the in-plane and bending node DOF; and $\lfloor H_u \rfloor$, $\lfloor H_v \rfloor$, and $\lfloor H_w \rfloor$ denote in-plane and transverse displacement shape functions, respectively.

The finite element formulation is based on the von Kármán large deflection and the laminated plate theories. The strain-displacement relations are given as

$$\{\varepsilon\} = \begin{Bmatrix} \varepsilon_x \\ \varepsilon_y \\ \gamma_{xy} \end{Bmatrix} = \{\varepsilon^0\} + z\{\kappa\} = \begin{Bmatrix} \varepsilon_m^0 \end{Bmatrix} + \begin{Bmatrix} \varepsilon_\theta^0 \end{Bmatrix} + z\{\kappa\} \tag{2}$$

where

$$\begin{Bmatrix} \varepsilon_m^0 \end{Bmatrix} = \begin{Bmatrix} u_{,x} \\ v_{,y} \\ u_{,y} + v_{,x} \end{Bmatrix} = [B_m]\{w_m\} \tag{3}$$

$$\begin{Bmatrix} \varepsilon_\theta^0 \end{Bmatrix} = \frac{1}{2}\begin{Bmatrix} w_{,x}^2 \\ w_{,y}^2 \\ 2w_{,x}w_{,y} \end{Bmatrix} = \frac{1}{2}\begin{bmatrix} w_{,x} & 0 \\ 0 & w_{,y} \\ w_{,y} & w_{,x} \end{bmatrix}\begin{Bmatrix} w_{,x} \\ w_{,y} \end{Bmatrix} = \frac{1}{2}[\theta][B_\theta]\{w_b\} \tag{4}$$

$$\{\kappa\} = \begin{Bmatrix} -w_{,xx} \\ -w_{,yy} \\ -2w_{,xy} \end{Bmatrix} = [B_b]\{w_b\} \tag{5}$$

where $\{\varepsilon^0\}$ and $\{\kappa\}$ denote the in-plane strain and curvature strain vectors and $[\theta]$ is the slope matrix, respectively. The matrices $[B_m]$, $[B_\theta]$, and $[B_b]$ are the strain interpolation matrices corresponding to in-plane, large deflection, and bending strain components, respectively.[15] The variable z is the distance from the midsurface of the plate. The subscripts m, θ, and b denote that the strain components are caused by membrane, large deflection, and bending, respectively; and the comma denotes the derivative.

The stress–strain constitutive relations for the kth lamina with a general orientation angle and a temperature change are

$$\{\sigma\}_k = \begin{Bmatrix} \sigma_x \\ \sigma_y \\ \tau_{xy} \end{Bmatrix}_k = \begin{bmatrix} Q_{11} & Q_{12} & Q_{16} \\ Q_{21} & Q_{22} & Q_{26} \\ Q_{61} & Q_{62} & Q_{66} \end{bmatrix}_k \left(\begin{Bmatrix} \varepsilon_x \\ \varepsilon_y \\ \gamma_{xy} \end{Bmatrix} - \Delta T \begin{Bmatrix} \alpha_x \\ \alpha_y \\ \alpha_{xy} \end{Bmatrix}_k \right) \tag{6a}$$

or

$$\{\sigma\}_k = [Q]_k(\{\varepsilon\} - \Delta T\{\alpha\}_k) \tag{6b}$$

where $[Q]_k$ is the transformed reduced stiffness matrix and $\{\alpha\}_k$ is the thermal expansion coefficient vector.

The resultant forces and moments per unit length are

$$(\{N\}, \{M\}) = \int_{-h/2}^{h/2} \{\sigma\}_k(1, z)\, dz \tag{7}$$

and the constitutive equations for a laminate can be written as

$$\begin{Bmatrix} N \\ M \end{Bmatrix} = \begin{bmatrix} A & B \\ B & D \end{bmatrix}\begin{Bmatrix} \varepsilon^0 \\ \kappa \end{Bmatrix} - \begin{Bmatrix} N_{\Delta T} \\ M_{\Delta T} \end{Bmatrix} \tag{8}$$

where $[A]$, $[B]$, and $[D]$ are the laminate extensional, extension-bending, and bending stiffness matrices, respectively. The vectors $\{N_{\Delta T}\}$ and $\{M_{\Delta T}\}$ are the in-plane force and moment caused by thermal expansion

$$(\{N_{\Delta T}\}, \{M_{\Delta T}\}) = \int_{-h/2}^{h/2} [Q]_k \Delta T\{\alpha\}_k(1, z)\, dz \tag{9}$$

Using the principle of virtual work, the element nonlinear equations of motion are derived with the internal and external virtual work as

$$\delta W_{\text{int}} = \int_A (\{\delta\varepsilon^0\}^T\{N\} + \{\delta\kappa\}^T\{M\})\, dA$$

$$\delta W_{\text{ext}} = \int_A \{\delta w[p(x, y, t) - \rho h w_{,tt}] - \delta u(\rho h u_{,tt}) - \delta v(\rho h v_{,tt})\}\, dA \tag{10}$$

and the element equations of motion can be expressed as

$$\begin{bmatrix} m_b & 0 \\ 0 & m_m \end{bmatrix}\begin{Bmatrix} \ddot{w}_b \\ \ddot{w}_m \end{Bmatrix} + \left(\begin{bmatrix} k_b & k_B \\ k_B^T & k_m \end{bmatrix} - \begin{bmatrix} k_{N\Delta T} & 0 \\ 0 & 0 \end{bmatrix} \right)\begin{Bmatrix} w_b \\ w_m \end{Bmatrix} + \left(\begin{bmatrix} k_{1\text{Nm}} + k_{1\text{NB}} & k_{1\text{bm}} \\ k_{1\text{mb}} & 0 \end{bmatrix} + \begin{bmatrix} k_{2b} & 0 \\ 0 & 0 \end{bmatrix} \right)\begin{Bmatrix} w_b \\ w_m \end{Bmatrix} = \begin{Bmatrix} p_{b\Delta T} \\ p_{m\Delta T} \end{Bmatrix} + \begin{Bmatrix} p_b(t) \\ 0 \end{Bmatrix} \tag{11}$$

The subscripts B, $N\Delta T$, Nm, and NB denote that the corresponding stiffness matrix is caused by the laminate extension bending $[B]$, in-plane force components $\{N_{\Delta T}\}$, $\{N_m\}(= [A]\{\varepsilon_m^0\})$, and $\{N_B\}$ $(= [B]\{k\})$, respectively.

Assembling all of the elements and taking into account the kinematic boundary conditions, the system equations of motion in physical DOF can be expressed as

$$\begin{bmatrix} M_b & 0 \\ 0 & M_m \end{bmatrix}\begin{Bmatrix} \ddot{W}_b \\ \ddot{W}_m \end{Bmatrix} + \left(\begin{bmatrix} K_b & K_B \\ K_B^T & K_m \end{bmatrix} - \begin{bmatrix} K_{N\Delta T} & 0 \\ 0 & 0 \end{bmatrix} \right)\begin{Bmatrix} W_b \\ W_m \end{Bmatrix} + \left(\begin{bmatrix} K_{1\text{Nm}} + K_{1\text{NB}} & K_{1\text{bm}} \\ K_{1\text{mb}} & 0 \end{bmatrix} + \begin{bmatrix} K_{2b} & 0 \\ 0 & 0 \end{bmatrix} \right)\begin{Bmatrix} W_b \\ W_m \end{Bmatrix} = \begin{Bmatrix} P_{b\Delta T} \\ P_{m\Delta T} \end{Bmatrix} + \begin{Bmatrix} P_b(t) \\ 0 \end{Bmatrix} \tag{12a}$$

or

$$[M]\{\ddot{W}\} + ([K] - [K_{N\Delta T}] + [K_1] + [K_2])\{W\} = \{P_{\Delta T}\} + \{P(t)\} \tag{12b}$$

where $[M]$, $[K]$, and $\{P\}$ denote the system mass, linear stiffness matrices, and load vector, respectively; and $[K_1]$ and $[K_2]$ denote the first-order and second-order nonlinear stiffness matrices, which depend linearly and quadratically on displacement $\{W\}$. The damping effect is difficult to model and quantify in physical DOF. Therefore, it is neglected in Eq. (12), and it will be discussed and added when modal equations are introduced.

For a given temperature rise ΔT Eq. (12) can be solved by numerical integration with simulated random loads. This turned out to be computationally costly because 1) of the large number of DOF of the system, 2) of the nonlinear stiffness matrices $[K_1]$ and $[K_2]$ have to be assembled and updated from the element nonlinear stiffness matrices at each time step, and 3) the time step of integration has to be extremely small. Consequently, Eq. (12) is transformed into modal equations by using a set of truncated modal coordinates.

Equations of Motion in Modal Coordinates

For symmetrically laminated composite and isotropic panels the laminate coupling stiffness $[B]$ is null, and the two submatrices in Eq. (12) are

$$[K_B] = [K_{1\mathrm{NB}}] = 0 \tag{13}$$

By neglecting the membrane inertia term, the membrane displacement vector can be expressed in terms of the bending displacement vector as

$$\{W_m\} = [K_m]^{-1}(\{P_{m\Delta T}\} - [K_{1\mathrm{mb}}]\{W_b\}) \tag{14}$$

Then Eq. (12) can be written in terms of the bending displacement as

$$\begin{aligned}[M_b]\{\ddot{W}_b\} &+ ([K_b] - [K_{N\Delta T}])\{W_b\} + [K_{1\mathrm{bm}}][K_m]^{-1}\{P_{m\Delta T}\} \\ &+ [K_{1\mathrm{Nm}}]\{W_b\} + \left([K_{2b}] - [K_{1\mathrm{bm}}][K_m]^{-1}[K_{1\mathrm{mb}}]\right)\{W_b\} \\ &= \{P_{b\Delta T}\} + \{P_b(t)\}\end{aligned} \tag{15}$$

Assuming that the panel deflection can be expressed as a linear combination of some known base functions as

$$\{W_b\} = \sum_{r=1}^{n} q_r(t)\{\phi_b\}^{(r)} = [\phi]\{q\} \tag{16}$$

where $\{\phi_b\}^{(r)}$ corresponds to the normal modes of the linear vibration problem

$$\omega_r^2[M_b]\{\phi_b\}^{(r)} = [K_b]\{\phi_b\}^{(r)} \tag{17}$$

Based on modal reduction, it is necessary to transform all of the nonlinear stiffness matrices in Eq. (15) into modal coordinates. The nonlinear stiffness matrices $[K_{1\mathrm{bm}}]$ and $[K_{2b}]$ are both in function of $\{W_b\}$; they can be expressed as the sum of products of modal coordinates and nonlinear modal stiffness matrices as

$$\begin{aligned}[K_{1\mathrm{bm}}] &= [K_{1\mathrm{mb}}]^T = \sum_{r=1}^{n} q_r(t)[K_{1\mathrm{bm}}(\phi_b)]^{(r)} \\ [K_{2b}] &= \sum_{r=1}^{n}\sum_{s=1}^{n} q_r(t)q_s(t)[K_{2b}\phi_b]^{(rs)}\end{aligned} \tag{18}$$

where the superindexes of those nonlinear modal stiffness matrices denote that they are assembled from the corresponding element nonlinear stiffness matrices. Those nonlinear stiffness matrices are evaluated with the corresponding element components $\{w_b\}^{(r)}$ obtained from the known system mode $\{\phi_b\}^{(r)}$.

The nonlinear stiffness matrix $[K_{1\mathrm{Nm}}]$ is linearly dependent on the displacement $\{W_m\}$. Recalling the membrane displacement vector of Eq. (14)

$$\begin{aligned}\{W_m\} &= [K_m]^{-1}(\{P_{m\Delta T}\} - [K_{1\mathrm{mb}}]\{W_b\}) \\ &= [K_m]^{-1}\left(\{P_{m\Delta T}\} - \sum_{r=1}^{n}\sum_{s=1}^{n} q_r(t)q_s(t)[K_{1\mathrm{mb}}]^{(r)}\{\phi_b\}^{(s)}\right) \\ &= \{W_m\}_{\Delta T} - \sum_{r=1}^{n}\sum_{s=1}^{n} q_r(t)q_s(t)\{\phi_m\}^{(rs)}\end{aligned} \tag{19}$$

It is observed that $[K_{1\mathrm{Nm}}]$ is the sum of two matrices: the first $[K_{\mathrm{Nm}}]_{\Delta T}$ is evaluated with $\{W_m\}_{\Delta T}(= [K_m]^{-1}\{P_{m\Delta T}\})$, and the second $[K_{2\mathrm{Nm}}]$ is evaluated with $\{\phi_m\}^{(rs)}(= [K_m]^{-1}[K_{1\mathrm{mb}}]^{(r)}\{\phi_b\}^{(s)})$, as

$$[K_{1\mathrm{Nm}}] = [K_{\mathrm{Nm}}]_{\Delta T} - \sum_{r=1}^{n}\sum_{s=1}^{n} q_r(t)q_s(t)[K_{2\mathrm{Nm}}(\phi_m)]^{(rs)} \tag{20}$$

Introducing a structural modal damping $2\xi_r\omega_r M_r[I]$, where the modal damping ξ_r, can be based on experimental data or selected from a similar structure employed previously. The equations of motion (15) are reduced to a set of coupled modal equations as

$$[M]\{\ddot{q}\} + 2\xi_r\omega_r M_r[I]\{\dot{q}\} + ([K_L] + [K_{\mathrm{qq}}])\{q\} = \{P\} \tag{21}$$

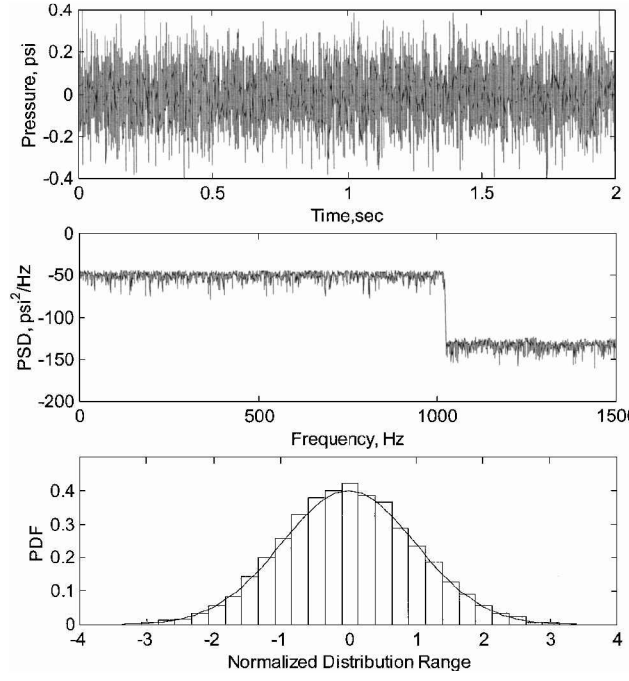

Fig. 1 Simulation of band-limited white noise.

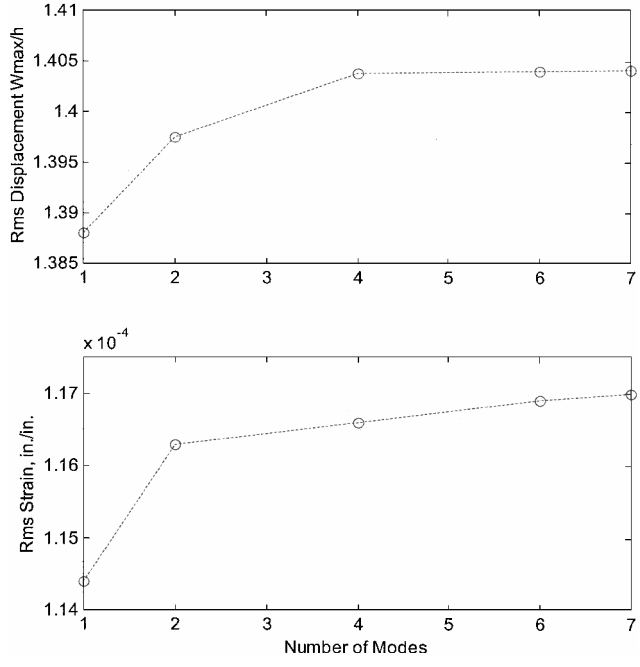

Fig. 2 Convergence of rms displacement and strain for a simply supported isotropic plate at 120-dB SPL.

where the diagonal modal mass is

$$[\bar{M}] = [\phi]^T [M_b][\phi] = \bar{M}_r[I] \tag{22}$$

the linear and cubic terms are

$$[\bar{K}_L]\{q\} = [\phi]^T([K_b] - [K_{N\Delta T}] + [K_{\mathrm{Nm}}]_{\Delta T})[\phi]\{q\} + [\phi]^T \sum_{r=1}^{n} q_r [K_{1\mathrm{bm}}]^{(r)} \{W_m\}_{\Delta T} \tag{23}$$

$$[\bar{K}_{\mathrm{qq}}]\{q\} = [\phi]^T \sum_{r=1}^{n}\sum_{s=1}^{n} q_r q_s \Big([K_{2b}]^{(rs)} - [K_{2\mathrm{Nm}}]^{(rs)} - [K_{1\mathrm{bm}}]^{(r)}[K_m]^{-1}[K_{1\mathrm{bm}}]^{(s)}\Big)[\phi]\{q\} = \sum_{r=1}^{n}\sum_{s=1}^{n} q_r q_s \big([\bar{K}_{\mathrm{qq}}]^{(rs)}\big)\{q\} \tag{24}$$

and the modal thermal and random load vector is

$$\{\bar{P}\} = [\phi]^T (\{P_{b\Delta T}\} + \{P_b(t)\}) \tag{25}$$

In Eq. (24) the nonlinear modal stiffness matrix $[\bar{K}_{\mathrm{qq}}]^{(rs)}$ is a constant matrix, so that the updating at each time step is not needed. The nonlinear random response for a given symmetric composite or isotropic panel at certain temperature can thus be determined from Eq. (21) by any numerical integration scheme. The Runge–Kutta scheme is employed in the present paper. The advantages of using the modal equations are 1) the number of modal equations is small (DOF of $\{q\}$ << DOF of $\{W_b\}$), 2) there is no need to assemble and update the nonlinear cubic term at each time step because all of the nonlinear modal stiffness matrices are constant matrices, and 3) the time step of integration could be larger because the maximum frequency of the truncated system is much lower. The method is applicable for both symmetric and unsymmetrical composite plates.[18] For unsymmetrical laminates formulation the reader is referred to Mei et al.[18]

Stress and Strain Calculations

After the modal displacement time history $\{q\}$ is determined for a given combination of acoustic load and elevated temperature case, the time histories of $\{W_b\}$ and $\{W_m\}$ can be evaluated with Eqs. (16) and (19) for the symmetric panels. The element in-plane strain $\{\varepsilon^0\}$ and curvature $\{\kappa\}$ can be calculated using Eqs. (3–5), respectively. The element strains are then obtained from Eq. (2), and stresses for the kth layer from Eq. (6). For

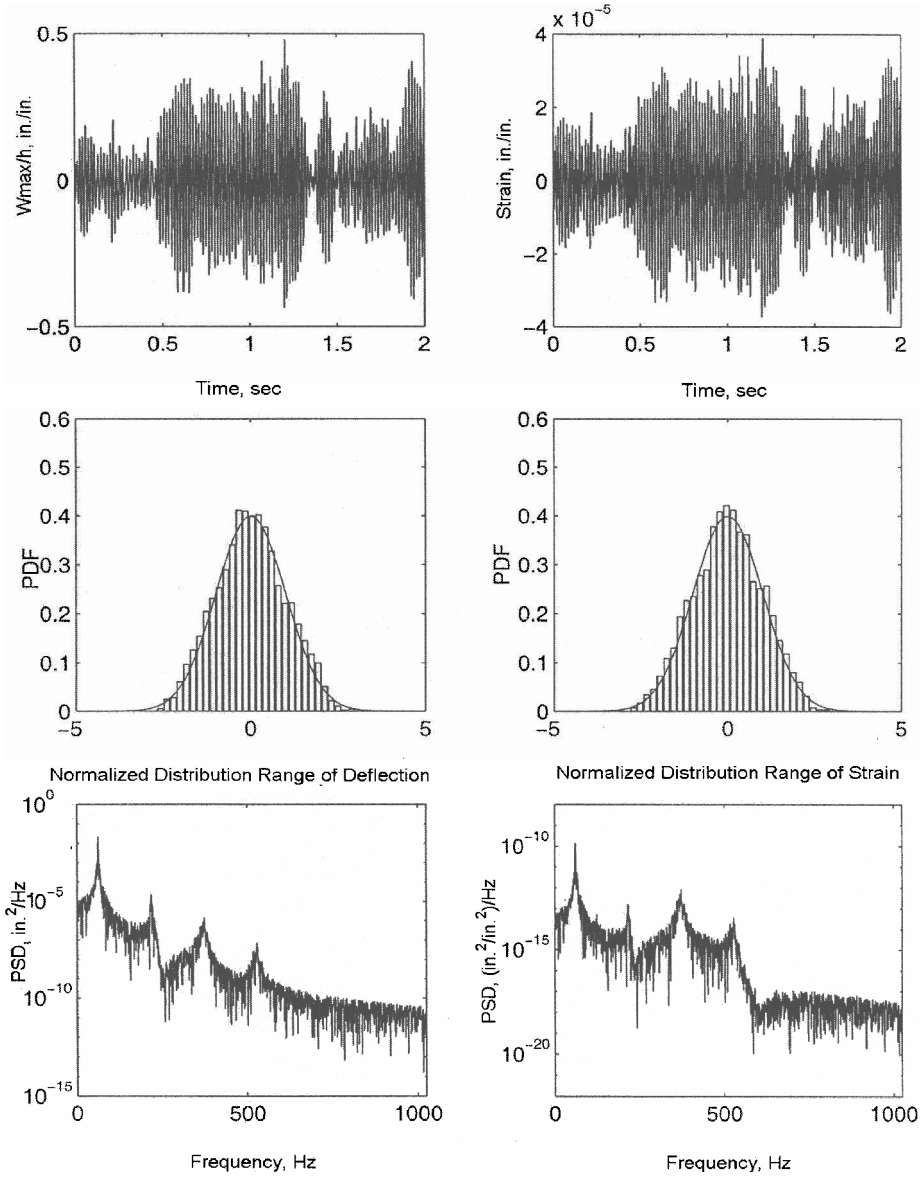

Fig. 3 Random response of a simply supported isotropic plate at SPL = 90 dB and $\Delta T = 0.0$.

the displacement-based finite element method the stress–strain calculation is not as accurate as displacement calculation. According to Barlow[19] and Cook et al.,[20] the stress–strain values at Barlow points are calculated, and the result is extrapolated to the nodal points or other desired points. The global stresses and strains are averaged from different local nodal values, which share the same global node number.

Acoustic Load Simulation

Consider a random pressure $p(x, y, t)$ acting on the surface of a high-speed flight vehicle. The pressure acting normal to the panel surface varies randomly in time and space along the surface coordinates x and y. The pressure $p(x, y, t)$ is characterized by a cross-spectral density function $S_p(\xi, \eta, \omega)$, where $\xi = x_1 - x_2$ and $\eta = y_1 - y_2$ are the spatial separations and ω is the frequency. The simplest form of the cross-spectral density is the truncated Gaussian random pressure uniformly distributed with spatial coordinates x and y.

$$S_p(\xi, \eta, f) = \begin{cases} S_0 & \text{if} \quad 0 \le f \le f_u \\ 0 & \text{if} \quad f < 0 \quad \text{or} \quad f > f_u \end{cases} \tag{26}$$

where S_0 is constant and f_u is the upper cutoff frequency. The expression for S_0 can be written as[8]

$$S_0 = p_0^2 10^{SPL/10} \tag{27}$$

where p_0 is the reference pressure, $p_0 = 2.90075 \times 10^{-9}$ psi (20 μPa), and SPL is the sound pressure level expressed in decibels. A typical simulated random load for the isotropic plate is shown in Fig. 1. The analyses presented are obtained for a cutoff frequency of 1024 Hz for the isotropic plate. For instance, for a uniformly Gaussian random load of 100 dB over a frequency range of 0–1024 Hz corresponds to an overall SPL of 130 dB.

Finite Element Validation

The nonlinear element equations developed in Eq. (11) are general in the sense that they are applicable for beam,[15,16] rectangular,[14,15,21] and triangular[17,22,23] plate finite elements. The finite element employed in the present study is the Bogner–Fox–Schmit[24] (BFS) C^1-conforming rectangular plate element. Each BFS element has a total of 24 DOF, 16 bending DOF $\{w_b\}$, and 8 in-plane DOF $\{w_m\}$.

Accurate nonlinear analytical multimode results and test data for panels under acoustic and thermal loads are not available in the literature. Validation of the present nonlinear modal formulation will thus consists of two parts: 1) nonlinear free vibrations to assess the accuracy of the left side of Eq. (21) with zero damping, and 2) linear random vibrations to validate the simulated random load $\{P\}$ at the right side of Eq. (21) with $\Delta T = 0$. The accuracy of the nonlinear stiffness matrices in modal coordinates has been verified by Shi et al.[25] for nonlinear free vibration of fundamental and higher modes of plates and beams. The validation of simulated random loads is by comparison of the linear displacements with

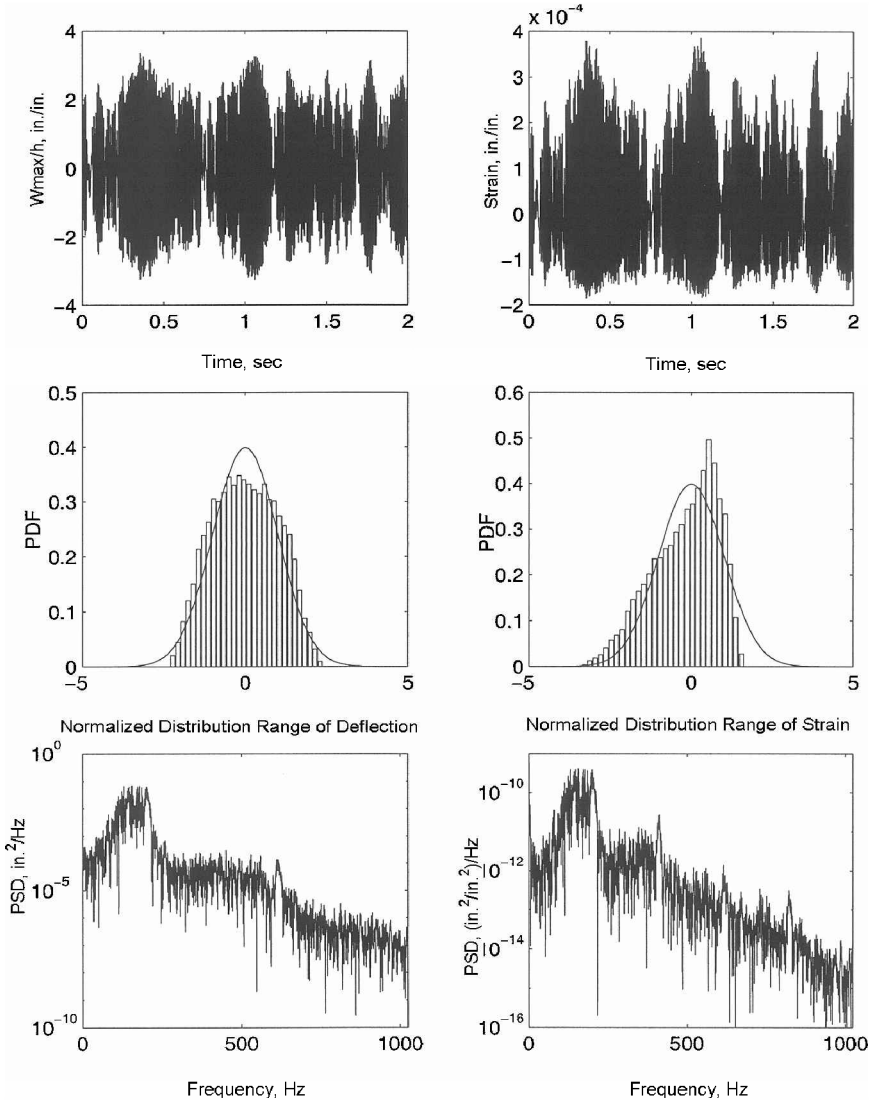

Fig. 4 Random response of a simply supported isotropic plate at SPL = 120 dB and $\Delta T = 0.0$.

linear analytical results[26] for a simply supported $15 \times 12 \times 0{\cdot}040$ in. ($38{\cdot}1 \times 30{\cdot}5 \times 0{\cdot}1$ cm) aluminum plate shown in Table 1. The material properties are $E = 10{\cdot}587 \times 10^6$ psi (73 GPa), $\nu = 0{\cdot}3$, $\rho = 2{\cdot}588 \times 10^{-4}$ lbf-s^2/in.^{4} (2763 kg/m^3) and the thermal expansion coefficient $\alpha = 6{\cdot}5 \times 10^{-6}/^\circ$F ($11{\cdot}7 \times 10^{-6}/^\circ$C). The FPK method is an exact solution[5,27] to the single-DOF forced Duffing equation under stationary, Gaussian excitations. The present time-domain numerical simulation results are shown in Table 2. Although the FPK method is applied with pure white noise, although finite element simulation has to use band-limited white noise, they showed good agreement, especially between FPK and FE four-mode results. The natural frequencies of the lowest seven modes in ascending order are given in Table 3.

Numerical Results

A simply supported rectangular plate with immovable in-plane conditions $u(0, y) = u(a, y) = v(x, 0) = v(x, b) = 0$ is studied in detail. The plate is of $14 \times 10 \times 0{\cdot}040$ in. ($35{\cdot}6 \times 25{\cdot}4 \times 0{\cdot}1$ cm) and is modeled with a 14×10 mesh (140 BFS elements) in a quarter-plate. The material properties are the same as those just mentioned. A proportional damping ratio of $\xi_r \omega_r = \xi_s \omega_s$ is used, and the fundamental modal damping coefficient ξ_1 is set to 0.02. The lowest seven natural frequencies are given in Table 4, which will be used to select the cutoff frequency used in the simulation.

Table 1 Comparison of rms W_{max}/h of linear analysis between analytical and FE results for a simply supported $38{\cdot}1 \times 30{\cdot}5 \times 0{\cdot}1$ cm isotropic plate

	Linear analytical	Linear FE	
SPL, dB	Four modes	Four modes	Err., %
90	0.2759	0.2760	0.0362
100	0.8725	0.8728	0.0362
110	2.7590	2.7600	0.0362
120	8.7248	8.7281	0.0362

Table 2 Comparison of rms W_{max}/h of nonlinear analysis between FPK and FE results for a simply supported $38{\cdot}1 \times 30{\cdot}5 \times 0{\cdot}1$ cm isotropic plate

	FPK[5,27]	FE	
SPL, dB	One mode	One mode	Four modes
90	0.249	0.174	0.266
100	0.592	0.556	0.578
110	1.187	1.101	1.432
120	2.200	1.914	2.572

Table 3 Natural frequencies (Hz) of a simply supported $38{\cdot}1 \times 30{\cdot}5 \times 0{\cdot}1$ cm isotropic plate[a]

Mode	(1, 1)	(3, 1)	(1, 3)	(3, 3)	(5, 1)	(5, 3)	(1, 5)
Exact	44.078	181.68	259.09	396.70	456.90	671.91	689.12
FE	44.082	181.70	259.10	396.75	457.02	672.06	689.29

[a]Mesh size is 10×10 in a quarter-plate model; Exact frequencies from Levy's solution.

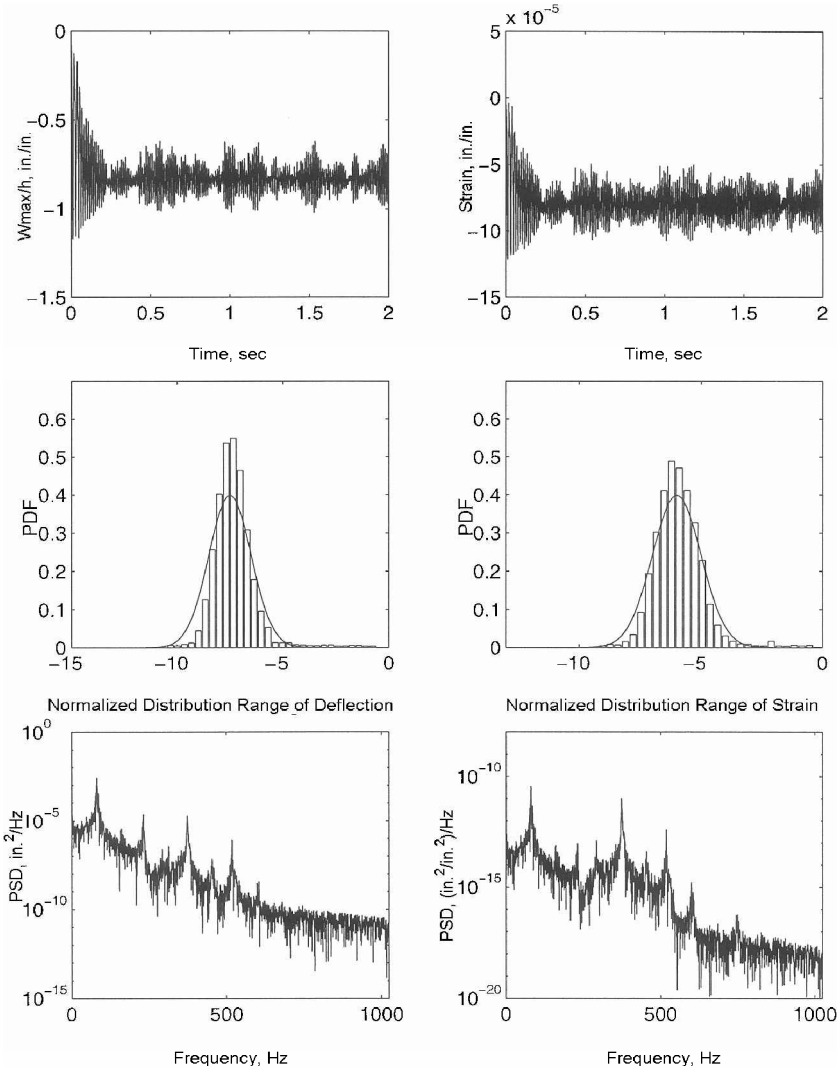

Fig. 5 Random response of a simply supported isotropic plate at SPL = 90 dB and $\Delta T/\Delta T_{cr} = 2.0$.

The number of modal coordinates to be included in the analyses for converged deflection and strain solutions are studied first. The rms maximum nondimensional deflection and the rms maximum strain vs numbers of modes at 120 dB SPL using 1, 2, 4, 6, and 7 modes are shown in Fig. 2. The maximum strain $\varepsilon_{y\,\max}$ is ε_y located at the plate center. The results show that four modes will give converged deflection and strain responses.

To eliminate the initial transient response, the first 0.5-s time history is excluded out of the statistical process. For more accurate statistical results the number of ensemble averages is taken as 10 for the present example. The linear frequency for the fourth mode (3, 3) is 523 Hz, and so the cutoff frequency for this simulation is selected as 1024 Hz, which is large enough to cover the shifted frequency caused by nonlinear effects.

Two other studies for accurate and converged response predictions are also performed. They are the finite element mesh sizes and the integration time steps. For a four-mode solution it was found that a quarter-plate model of 14×10 mesh size is adequate. The time step of integration $1/8192 = 1.2207 \times 10^{-4}$ s was first selected, then the time step was cut into one-half. The time histories for the two time steps were found to be exactly identical. Thus, the time step of 1/8192 s is used. Four modes are thus used in the results for the isotropic plate shown in the following: The time histories, probability density function, and power spectral density (PSD) of maximum deflection and strain at SPL = 90 and 120 dB and $\Delta T = 0{\cdot}0$ are shown in Figs. 3 and 4, and at SPL = 90, 100, and 120 dB and $\Delta T/\Delta T_{cr} = 2{\cdot}0$ ($\Delta T_{cr} = 2{\cdot}352^{\circ}$F for this plate) are shown in

Table 4 Natural frequencies (Hz) of a simply supported $35.6 \times 25.4 \times 0.1$ cm isotropic plate[a]

Mode	(1, 1)	(3, 1)	(1, 3)	(3, 3)	(5, 1)	(5, 3)	(1, 5)
Exact	58.116	215.19	365.98	523.05	529.33	837.19	981.70
FE	58.116	215.19	365.98	523.06	529.36	837.22	981.94

[a]Mesh size is 14×10-in a quarter-plate model; Exact frequencies from Levy's solution.

Table 5 Moments of W_{max}/h for the $35.6 \times 25.4 \times 0.1$ cm isotropic plate

SPL, DB	$\Delta T/\Delta T_{cr}$	rms	Mean	Variance	Skewness	Kurtosis
90	0.0	0.1608	1.241×10^{-4}	0.0258	0.0242	−0.4320
120	0.0	1.4039	-2.628×10^{-3}	1.9714	0.00634	−0.8613
90	2.0	0.8239	−0.8163	0.0124	2.0074	9.4296
100	2.0	0.7470	−0.1052	0.5470	−0.2480	−1.3823
120	2.0	1.5770	1.999×10^{-3}	2.4873	0.00272	−0.7367

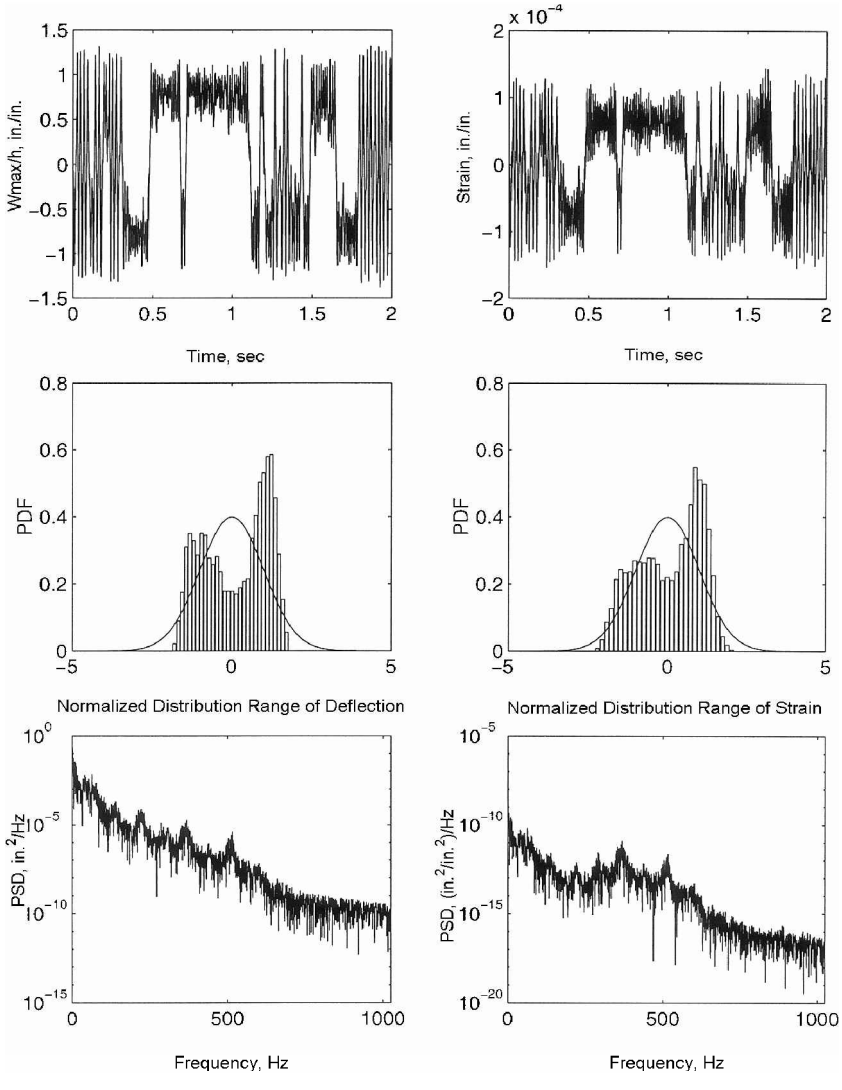

Fig. 6 Random response of a simply supported isotropic plate at SPL = 100 dB and $\Delta T/\Delta T_{cr} = 2.0$.

Table 6 Moments of $\varepsilon_{y\ max}$ for the 35.6 × 25.4 × 0.1 cm isotropic plate

SPL, DB	$\Delta T/\Delta T_{cr}$	rms	Mean	Variance	Skewness	Kurtosis
90	0.0	1.324×10^{-5}	−0.0176	0.000175	−0.0432	−0.4050
120	0.0	1.167×10^{-4}	22.268	0.01312	0.5744	0.4317
90	2.0	4.035×10^{-5}	−39.094	0.000333	0.22477	0.1467
100	2.0	6.612×10^{-5}	21.692	0.003902	0.26784	−1.2727
120	2.0	19.02×10^{-5}	72.950	0.031171	−0.5501	−0.1875

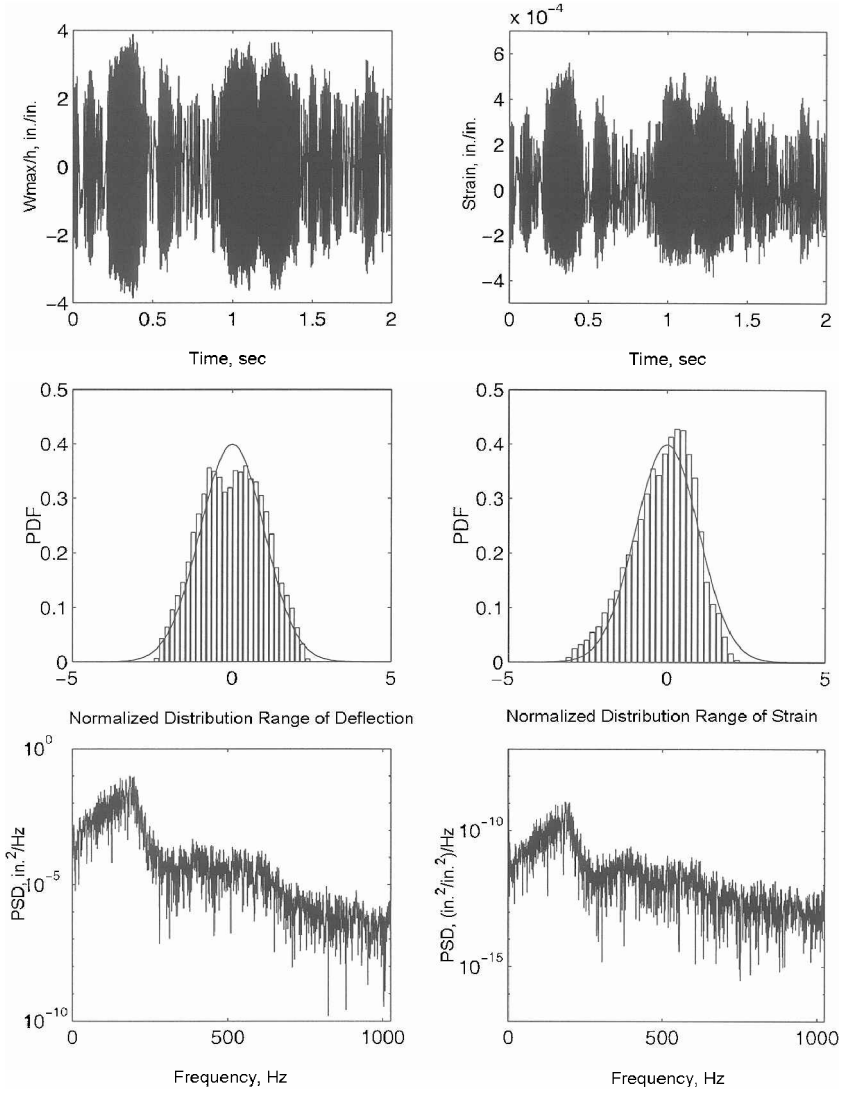

Fig. 7 Random response of a simply supported isotropic plate at SPL = 120 dB and $\Delta T/\Delta T_{cr} = 2.0$.

Figs. 5–7, respectively. Tables 5 and 6 give the statistical moments of the maximum deflection and maximum strain responses, respectively. The skewness and kurtosis coefficients are defined as

$$\text{Skewness} = \mu_3 / \sigma^3 \tag{28}$$

$$\text{Kurtosis} = \left(\mu_4 / \sigma^4\right) - 3 \tag{29}$$

where μ_k and σ are the kth central moment and standard deviation, respectively.

For the $\Delta T = 0$ results, at the low 90-dB SPL the plate behaves basically as small-deflection ($W_{max}/h = 0{\cdot}1608$) random vibration dominated by the fundamental (1, 1) mode as shown in the PSD plots of Fig. 3. The probability distributions for deflection and strain are both close to Gaussian. The time history at the high 120-dB SPL in Fig. 4 is clearly a large deflection ($W_{max}/h > 1{\cdot}0$) nonlinear random. This is demonstrated by the peaks in PSD plots that are broadening and shifting to the higher frequency and by the presence of a nonzero mean in-plane strain shown in the strain plots. The large deviation from the Gaussian is shown by the strain PDF and the large skewness and kurtosis values for strain in Table 6.

For combined acoustic and thermal loads the panel response indicates the three distinct types of motion of 1) small-deflection random vibration about one of the two thermally buckled equilibrium positions in Fig. 5, 2) snap-through or oil-canning phenomenon between the two buckled positions in Fig. 6, and 3) large-amplitude nonlinear random vibration covering both thermally buckled positions shown in Fig. 7. At low 90 dB and $\Delta T/\Delta T_{cr} = 2{\cdot}0$ the time histories in Fig. 5 show clearly the linear random responses about one of the thermally buckled positions of $(W_{max}/h)_{\Delta T} = -0{\cdot}8163$. The deflection PSD plot shows the domination of the fundamental mode, and the strain PSD plot shows the equal contribution from the third mode. Also, note the general increase of the panel vibration frequencies, for example, from 58 Hz (Fig. 3 at $\Delta T = 0$) to 86 Hz (Fig. 5 at $\Delta T/\Delta T_{cr} = 2{\cdot}0$) for the fundamental mode. As the SPL increased to 100 dB, the time histories in Fig. 6 show that snap-through motions and the deflection PDF is non-Gaussian. At high SPL of 120 dB

in Fig. 7, the large deflection rms W_{max}/h is 1.5770, which covers both buckled positions of $(W_{max}/h)_{\Delta T} = \pm 0.8163$. Nonlinearities are further observed by the broadening and shifting of the peaks in the PSD plots.

For a clamped rectangular graphite-epoxy laminated plate of eight layers $[0/45/\_45/90]_s$, the random response is much similar as the isotropic plate case. The readers are referred to Ref. 18.

Conclusions

A new finite element time-domain modal formulation is presented for the prediction of nonlinear random response of composite panels subjected to acoustic pressure at elevated temperature. The modal formulation is computationally efficient so that 1) the number of modal equations is small, 2) the nonlinear modal stiffness matrices are constant matrices, and 3) the time step of integration could be reasonably large. It is demonstrated that all three types of panel motion—1) linear random vibration about one of the buckled equilibrium position, 2) snap-through motions between the two buckled positions, and 3) nonlinear random response over both buckled positions—can be accurately predicted.

Acknowledgment

The first three authors would like to acknowledge the support by U.S. Air Force Research Laboratory, AFRL contract F33615-98-D-3210 No. 5.

References

[1]Clarkson, B. L., "Review of Sonic Fatigue Technology," NASA CR-4587, April 1994.

[2]Wolfe, H. F., Shroger, C. A., Brown, D. L., and Simmons, L. W., "An Experimental Investigation of Nonlinear Behavior of Beams and Plates Excited to High Levels of Dynamic Response," Wright Lab., WL-TR-96-3057, Wright–Patterson AFB, OH, Oct. 1995.

[3]Istenes, R. R., Rizzi, S. A., and Wolfe, H. F., "Experimental Nonlinear Random Vibration Results of Thermally Buckled Composite panels," *Proceedings of 36th Structures, Structural Dynamics, and Materials Conference*, AIAA, Washington, DC, April 1995, pp. 1559–1568.

[4]Iwan, W. D., and Yang, M. I., "Application of Statistical Linearization Techniques to Nonlinear Multi-Degree of Freedom Systems," *Journal of Applied Mechanics*, Vol. 39, June 1972, pp. 545–550.

[5]Bolotin, V. V., *Random Vibration of Elastic Systems*, Martinus–Nijhoff, The Hague, 1984, pp. 290–292.

[6]Shinozuka, M., and Jan, C.-M., "Digital Simulation of Random Processes and Its Applications," *Journal of Sound and Vibration*, Vol. 25, No. 1, 1972, pp. 111–128.

[7]Shinozuka, M., and Wen, Y. K., "Monte Carlo Solution of Nonlinear Vibrations," *AIAA Journal*, Vol. 10, No. 1, 1972, pp. 37–40.

[8]Arnold, R. R., and Vaicaitis, R., "Nonlinear Response and Fatigue of Surface Panels by the Time Domain Monte Carlo Approach," WRDC-TR-90-3081, Wright–Patterson AFB, OH, May 1992.

[9]Vaicaitis, R., and Kavallieratos, P. A., "Nonlinear Response of Composite Panels to Random Excitation," *Proceedings of the 34th Structures Structural Dynamics, and Materials Conference*, AIAA, Washington, DC, April 1993, pp. 1041–1049.

[10]Vaicaitis, R., "Time Domain Approach for Nonlinear Response and Sonic Fatigue of NASP Thermal Protection Systems," *Proceedings of the 32nd Structures, Structural Dynamics, and Materials Conference*, AIAA, Washington, DC, April 1991, pp. 2685–2708.

[11]Elishakoff, I., and Zhang, X., "An Appraisal of Different Stochastic Linearization Techniques," *Journal of Sound and Vibrations*, Vol. 153, No. 2, 1992, pp. 370–375.

[12]Roberts, J. B., and Spanos, P. D., *Random Vibration of Statistical Linearization*, Wiley, New York, 1990, Chap. 6.

[13]Green, P. D., and Killey, A., "Time Domain Dynamic Finite Element Modeling in Acoustic Fatigue Design," *Proceedings of the 6th International Conference on Structural Dynamics*, edited by N. S. Ferguson, H. F. Wolfe, and C. Mei, Inst. of Sound and Vibration Research, Univ. of Southampton, U.K., ISVR, July 1997, pp. 1007–1026.

[14]Robinson, J. H., "Finite Element Formulation and Numerical Simulation of the Large Deflection Random Vibration of Laminated Composite Plates," M.S. Thesis, Dept. of Aerospace Engineering, Old Dominion Univ., Norfolk, VA, Aug. 1990.

[15]Locke, J. E., "A Finite Element Formulation for the Large Deflection Random Response of Thermally Buckled Structures," Ph.D. Dissertation, Dept. of Aerospace Engineering, Old Dominion Univ., Norfolk, VA, July 1988.

[16]Locke, J. E., and Mei, C., "A Finite Element Formulation for Large Deflection Random Response of Thermally Buckled Beams," *AIAA Journal*, Vol. 28, No. 12, 1990, pp. 2125–2131.

[17]Mei, C., and Chen, R. R., "Finite Element Nonlinear Random Response of Composite Panels of Arbitrary Shape to Acoustic and Thermal Loads Applied Simultaneously," Wright Lab., WL-TR-97-3085, Wright–Patterson AFB, OH, Oct. 1997.

[18]Mei, C., Dhainaut, J. M., Duan, B., Spotswood, S. M., and Wolfe, H. F., "Nonlinear Random Response of Composite Panels in an Elevated Thermal Environment," U.S. Air Force Researh Lab., AFRL-VA-WP-TR-2000-3049, Wright–Patterson AFB, OH, Oct. 2000.

[19]Barlow, J., "Optimal Stress Locations in Finite Element Models," *International Journal for Numerical Methods in Engineering*, Vol. 10, No. 2, 1976, pp. 243–251.

[20]Cook, R. D., Malkus, D. S., and Plesha, M. E., Concepts and Applications of Finite Element Analysis, 3rd ed., Wiley, New York, 1989, p. 189.

[21]Shi, Y., and Mei, C., "Coexisting Thermal Postbuckling of Composite Plates with Initial Imperfections Using Finite Element Modal Methods," *Proceedings of the 37th Structures, Structural Dynamics, and Materials Conference*, AIAA, Reston, VA, April 1996, pp. 1355–1362.

[22]Xue, D. Y., "A Finite Element Frequency Domain Solution of Nonlinear Panel Flutter with Temperature Effects and Fatigue Life Analysis," Ph.D. Dissertation, Dept. of Mechanical and Engineering Mechanics, Old Dominion Univ., Norfolk, VA, March 1991.

[23]Xue, D. Y., and Mei, C., "Finite Element Nonlinear Panel Flutter with Arbitrary Temperatures in Supersonic Flow," *AIAA Journal*, Vol. 31, No. 1, 1993, pp. 154–162.

[24]Bogner, F. K., Fox, R. L., and Schmit, L. A., "The Generation of Inter-Element Compatible Stiffness and Mass Matrices by the Use of Interpolation Formulas," AFFDL-TR-66-80, Wright–Patterson AFB, OH, Nov. 1996, pp. 396–443.

[25]Shi, Y., Lee, R., and Mei, C., "A Finite Element Multimode Method to Nonlinear Free Vibrations of Composite Plates," *AIAA Journal*, Vol. 35, No. 1, 1997, pp. 159–166.

[26]Lutes, L. D., and Sarkani, S., *Stochastic Analysis of Structural and Mechanical Vibrations*, Prentice–Hall, Upper Saddle River, NJ, 1997, pp. 227–235.

[27]Chiang, C. K., "A Finite Element Large Deflection Multi-Mode Random Response Analysis of Complex Panels with Initial Stresses Subjected to Acoustic Loading," Ph.D. Dissertation, Dept. of Mechanical and Engineering Mechanics, Old Dominion Univ., Norfolk, VA, Dec. 1988.